Annals of Glaciology 6 1985

ENCLOSURE OF AIR DURING METAMORPHOSIS OF DRY FIRN TO ICE

by

B. Stauffer, J. Schwander and H. Oeschger

Physics Institute, University of Bern, Switzerland

ABSTRACT

If cold firn has reached a density of about 0.55 Mg m^{-3}, further densification occurs by a sintering process which increases the contact surface between the firn grains. The pore volume is decreasing continuously but the firn remains permeable to air up to a density of 0.82 Mg m^{-3}. At about this density the remaining air in the pore volume is closed off in isolated bubbles. We are interested in the age and the age distribution of the air enclosed in bubbles relative to the age of the surrounding ice, and are investigating the development of the pore volume in firn.

A newly constructed measuring device allows the field measurement of the amount of air which is already enclosed in bubbles of firn samples. Measurements have been made during summer 1983 in Greenland and during winter 1983/84 at the South Pole. The results are discussed and compared with results obtained with a simplified statistical sintering model, using some results of percolation theory.

INTRODUCTION

The presence of bubbles is one of the typical properties of natural ice. Air in bubbles of ice which was formed by sintering of dry firn has essentially the same composition as that of the atmosphere at the time of bubble formation. The analysis of dated ice samples therfore allows the investigation of the history of atmospheric composition (Delmas and others 1980; Berner and others 1980). The age of the enclosed air is, however, not the same as that of the surrounding ice since air bubbles become isolated from the atmosphere during the transition from firn to ice, occurring typically 100 to 3 000 years after snow deposition. The time needed to transform freshly deposited snow into ice depends mainly on firn temperature and snow accumulation rate. The mean age difference between ice and enclosed air, as well as the width of the age distribution for a given sample, depend on the enclosure process and on the age of the atmospheric air in the permeable firn. The enclosure process, investigated by measurements on firn samples and by computer simulations with a simplified sintering model, are discussed in this paper. Concerning the age in the permeable firn, we have some evidence that the air is well mixed with the atmosphere to a depth of several meters above the transition zone (Loosli 1983; Stauffer and others 1981). More measurements are needed to decide whether the air is well mixed down to the transition zone or not.

To investigate the enclosure process the fraction of air, which is already isolated from the atmosphere, has to be measured as a function of depth.

EXPERIMENTAL PROCEDURE

A widely applied method to measure the isolated fraction of air in a firn sample is to remove the air in the open pore space, melt the sample afterwards and measure the amount of gas extracted during melting of the sample (Langway 1958; Raynaud and Lebel 1979). Two methods have been used to remove the air from the open pore space: by evacuating the container with the firn sample or by immersing the sample slowly in a liquid which displaces the air in the open pore volume. The two methods do not give the same results. By evacuating the container containing the firn sample, there is some risk of breaking isolated but still fragile bubbles due to the high pressure difference between bubbles and the evacuated open pore space. By immersing the sample, air from open but dead-ended channels may not be removed.

To avoid these problems, we applied a classical method based on the law of Boyle-Mariotte for ideal gases. The measuring device is shown schematically in Figure 1. The three volumes V_1 (110.3 cm^3), V_2 (110.2 cm^3), and V_3 (12.7 cm^3) have been machined into one massive aluminium block to keep all three volumes at the same temperature.

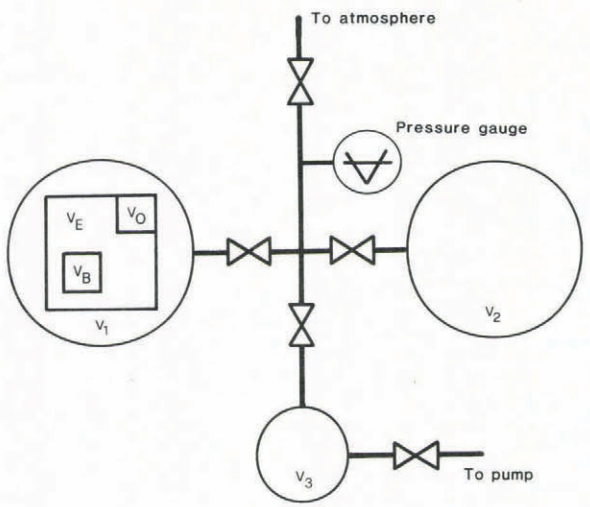

Fig.1. Schematic arrangement of system to measure the enclosed bubble volume of firn and ice samples.

The firn samples are cut on a small turntable to a cylindrical shape. The bulk volume about 35 cm^3 is determined by measuring length and diameter of the cylinder, accuracy 0.1‰. The weight is measured with an absolute accuracy of 0.02 g. The ice volume V_E is calculated using a density of 0.919 Mg m^{-3} for pure ice at -25 °C.

For the measurement, volume V_1 containing the firn sample is disconnected from the atmosphere and connected to V_3 which was evacuated previously. The pressure drop Δp_1 due to expansion is measured. Assuming an isothermal process, the bubble volume V_B can be calculated:

$$V_B = V_A - V_E$$

$$(p_A - \Delta p_1)(V_1 - V_A + V_3) = (V_1 - V_A)\, p_A \qquad (1)$$

where: p_A = atmospheric pressure

V_B = bubble volume

https://doi.org/10.3189/1985AoG6-1-108-112 Published online by Cambridge University Press

By measuring in a second step the pressure drop Δp_2 by connecting the calibrated volume V_2 at atmospheric pressure to V_3 which was evacuated again previously, we can replace p_A:

$$V_A = V_1 + V_3 - \frac{\Delta p_2}{\Delta p_1}(V_2 + V_3) \qquad (2)$$

Thus Δp_2, a pressure change of the same order as Δp_1, can be measured with the same instrument, instead of the atmospheric pressure, assuming that p_A remains constant during the two measurements.

The pressure drop Δp_1 is of the order of 5 000 Pa (0.05 bar). This small pressure change should exclude any danger of breaking fragile isolated bubbles.

The method has several possible error sources which are discussed in detail by Schwander (1984). An important correction involves the water vapour pressure. Equation 2 has to be corrected to:

$$V_A = V_1 + V_3 - \frac{\Delta p_2}{\Delta p_1}(V_2 + V_3) + p_w V_3 \cdot \left[\frac{1}{\Delta p_1} - \frac{V_3}{\Delta p_2 (V_2 + V_3)}\right] \qquad (3)$$

where: p_w = water vapour pressure.

A correction due to adiabatic cooling during expansion can be neglected, if the pressure readings are done 20 s after the expansion. The influence of the Joule-Thomson effect as well as the deviation of air from an ideal gas (Van der Vaals correction) can also be neglected.

The experimental method was tested with bubble free ice. The accuracy of the bulk density and bubble volume measurements are ± 0.002 Mg m^{-3} respectively ± 2 cm^3 kg^{-1}.

RESULTS

Measurements were done on a firn/ice core from Dye 3 (South Greenland, 65°11'N, 43°50'W) and on a core from Siple Station (West Antarctica, 75°55'S, 83°55'W). The measurements on the core from Dye 3 were done in summer 1983, the measurements on the core from Siple Station with improved equipment and under more favorable conditions in December 1983 in a snow trench at the South Pole. Results from the Siple core will be reported. The mean annual air temperature for this site is -24°C which minimizes the risk of an influence of the sintering process by meltwater. Only one melt-layer of 10 mm thickness was observed in the entire firn core. The high annual accumulation of about 0.5 Mg m^{-2} allows the study of seasonal effects. Counting the seasonal variations of the electrical conductivity of the ice core allows also a dating of the core over the last 200 years with an accuracy of ± 2 years (Schwander and Stauffer 1984).

Density and bubble volume of a total of 257 samples from 10 to 91 m depth below the 1982 snow surface were determined. Each point in Figure 2 represents the average of 10 measurements done on samples from a 1 m long ice core. Samples have been taken every 10 m to a depth of 60 m below surface. From 64 to 81 m 182 samples of 0.1 m length have been measured. The enclosure process mainly takes place in a depth interval between 64 m and 76 m. Only 10% of the final bubble volume is enclosed above 64 m and only 10% below 76 m. This depth interval is characteristic for Siple Station only. There is a clear dependence between density and bubble volume which is shown in Figure 3.

Figure 4 shows all results of a small section of the Siple core. The bubble volume, as well as the bulk density, shows seasonal variations demonstrated by the comparison with electrical conductivity measurements. The summer layers at this depth are characterized by low density and low isolated bubble volume.

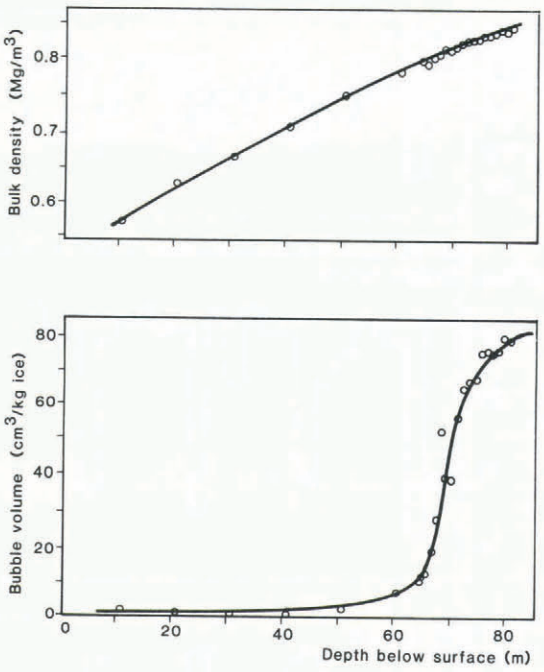

Fig.2. Bulk density and bubble volume versus depth at Siple Station. Each point represents a one meter average.

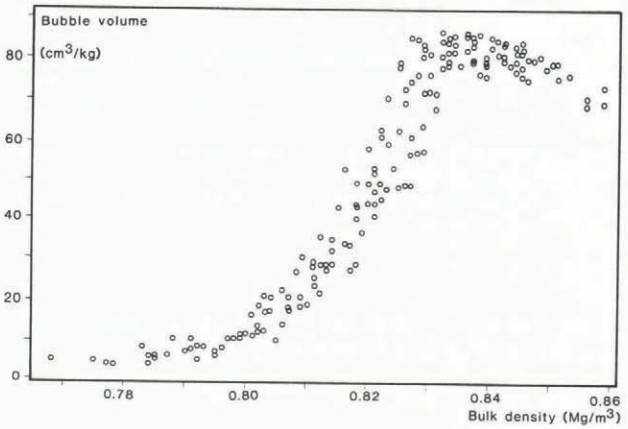

Fig.3. Bubble volume versus bulk density for all samples from Siple Station between 60 m and 81 m depth below surface.

DISCUSSION OF RESULTS

Bubble close-off occurs at different sites in different depth depending on accumulation rate and temperature, but at about the same mean density (Raynaud and Lebel 1979). Based on this observation, on measurements made on firn samples from North Central (Greenland) (Stauffer and others 1981), and due to results we obtained from the firn core from Dye 3, we make the hypothesis that the relation between isolated bubble volume and density, shown in Figure 3, is valid for all sites where ice is formed by sintering of dry firn. The isolated bubble volume is, however, not identical with the enclosed amount of gas since the pressure in bubbles is not uniform.

The pressure in the bubbles starts to increase above atmospheric as soon as the bubbles are closed-off since the hydrostatic pressure of the surrounding ice is higher. At Siple Station (elevation 1054 m a.s.l.) we expect a mean air content of the ice of 120 cm^3 (STP) kg^{-1} (Raynaud and Lebel 1979). At the end of the pore close-off, the measured bubble volume is only 80 cm^3 kg^{-1}. The mean pressure in the bubbles therefore has to be about 140 kPa (1.4 bar). The pressure, not uniform, is larger in bubbles isolated at shallow depth compared

https://doi.org/10.3189/1985AoG6-1-108-112 Published online by Cambridge University Press

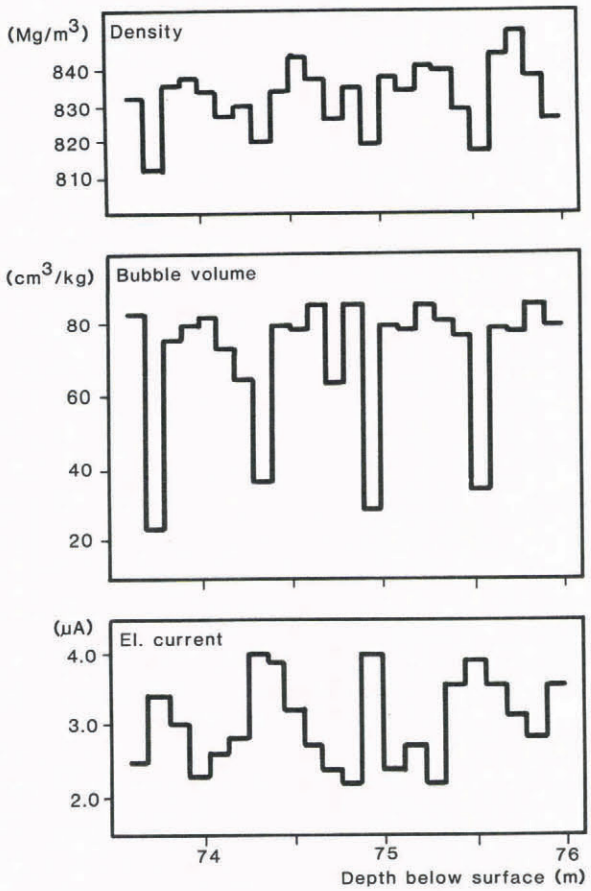

Fig.4. Detailed bulk density, bubble volume and electrical conductivity measurements for a section of firn core from Siple Station. High electrical conductivity is characteristic for summer layers.

to the pressure in bubbles enclosed at a deeper depth. The volume of isolated bubbles V_B is given by:

$$V_B(h_2) = \int_0^{h_2} V(h_1) \cdot B(h_1,h_2) \cdot dh_1 \qquad (4)$$

where: $V(h_1)\, dh_1$ = geometrical volume which is enclosed in depth interval dh_1.

$B(h_1, h_2)$ is the factor by which the volume enclosed at h_1 has been compressed when reaching the depth h_2. Schwander (1984) suggests an approximate solution, using a step function:

$$V_B(h_2) = B(h_1,h_2) \cdot V(h_1) \qquad (5)$$

where $V_B(h_2)$ and $V(h_1)$ are vectors, and $B(h_1,h_2)$ is a matrix. The elements of the matrix may be calculated if the compression of a bubble as a function of hydrostatic pressure and time is known. The compression formulae given by Wilkinson and Ashby (1975) have been used. The results depend on the shape of the bubbles. It is assumed that the shape is cylindrical after close off and becomes spherical after a few meters. Figure 5 shows the calculated enclosed amount of gas in function of depth. The depth interval needed to transform bubbles from a cylindrical into a spherical shape is the parameter. With 16 m depth interval the calculated amount of gas is 126 $cm^3\ kg^{-1}$ (corresponding to about 120 cm^3 (STP) kg^{-1}).

At 75 m depth summer layers are characterized by low density and low isolated bubble volume. Summer layers are, however, characterized by high air content

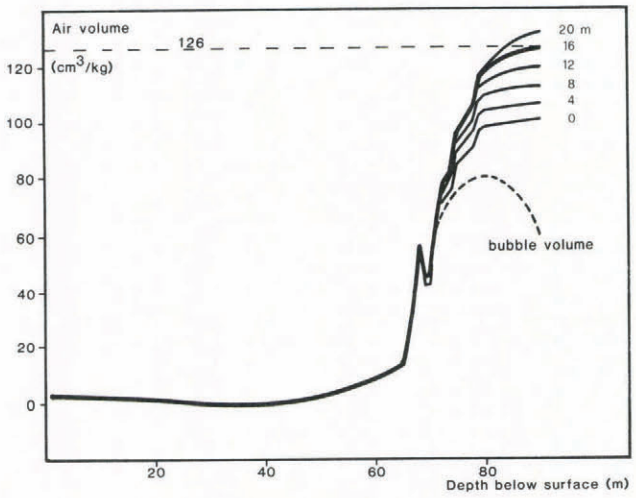

Fig.5. Calculated bubble volume (STP) assuming a mean atmospheric pressure of 867 mbar. The parameter is the mean depth interval needed to transform cylindric to spheric bubbles.

compared to winter layers (Berner and others 1979); Raynaud and Lebel 1979). We assume that impermeable winter layers are sealing permeable summer layers beneath with lower density and therefore higher porosity, against the atmosphere. The air in the summer layer cannot escape anymore and leads to a higher air content. An impermeable layer has a limited horizontal extension. The sealing effect is therefore only effective if the permeability of the layer beneath is reduced, still permeable over a distance typical for the layer thickness but impermeable over much larger horizontal distances.

COMPARISON WITH SIMPLIFIED STATISTICAL SINTERING MODEL

The sintering process of a powder compound is generally divided into three stages (Geguzin 1973). Contact areas between single grains are small in stage 1, while stage 2 is characterized by contact areas of the order of the cross section of the grains. Stage 3 is characterized by isolated bubbles. If density of firn is measured as a function of depth discontinuities are observed at densities of 0.55 Mg m^{-3} and 0.82 Mg m^{-3} (Anderson and Benson 1963). Maeno observed discontinuities of a few parameters at a density of 0.73 Mg m^{-3} (Maeno 1978). Firn grains of irregular shape and size are packed at random and have small contact areas at a density of 0.55 Mg m^{-3}. Spheres of uniform size packed analogic to a body centered lattice are considered to be a useful approximation to the irregular packing of firn grains. If the grains sinter together by enlarging the circular contact areas, their shape will change slowly from spheric to the shape of a tetrakaidekaeder (truncated octaeder). This shape is a good approximation of many shapes found in nature (Desch 1919). If the circular contact areas grow simultaneously, all channels connecting air pockets in the corners where four tetrakaidekaeders meet, will close simultaneously and isolate the remaining air in each corner (Stauffer 1981). Beere (1973) has calculated the remaining porosity approximately by assuming that the surface energy is the driving force. Observations of firn samples from a depth interval where bubbles are enclosed show that they are often present in small clusters with channels connecting them and that there are only one to two bubbles per grain (single crystal) (Gow 1968) instead of six as Beere's model would suggest.

Coble (19161) uses the same regular packing of grains but approximates the shape of the pore volume by cylindric channels going along with each boundary where three tetrakaidekaeder meet. A decrease of the porosity (increase of density) may occur by a decrease of the cylinder radius or by the closure of single

https://doi.org/10.3189/1985AoG6-1-108-112 Published online by Cambridge University Press

channels. Maeno suggests that the decrease of the diameter of the cylinders is dominant in sintering of firn until a density of 0.73 Mg m^{-3} is reached, and that further densification occurs by eliminating whole channels.

We assume for the following comparison that firn with a density of 0.73 Mg m^{-3} consists of a regular arrangement of regular tetrakaiderkaeders of uniform size and that the porosity consists of channels of uniform size and that there is such a channel at each boundary where three grains meet. The decreasing porosity accompanying a further densification shall be proportional to the decreasing number of channels. The idea is illustrated in Figure 6 with a two-dimensional hexagonal lattice. The bonds represent the air filled channels. The isolation of single bonds or clusters of bonds is a problem of bond percolation (Essam 1980). The probability P(p) that a certain bond is connected by a string of bonds with the surface is a uniformly increasing function of the probability p for the existence of single bonds. For a large number of bonds the probability p is identical with the remaining fraction of bonds and therefore proportional to porosity. For an infinite sample the probability P(b) that a bond is connected to an infinite cluster is zero if p is below the critical probability p_c. All bonds are therefore isolated in an infinite sample if p is below p_c, this corresponds with the transition from firn to ice. The critical probability for the two-dimensional hexagonal structure is $p_c = 0.653$ (Hammersley and Welsh 1980). for three-dimensional structures we found only the critical probability for the face centered cubic lattice in literature (Essam 1980): $p_c = 0.1185$. for the structure given by the edges of the tetrakaiderkaeders we estimate, based on computer simulations, that the critical probability is about $p_c = 0.42$.

The probability $p = 1$ corresponds to 100% channels between the tetrakaiderkaeders and therefore to a density of 0.73 Mg m^{-3} according to Maeno (1978). The porosity Π resp. Π' is related to density:

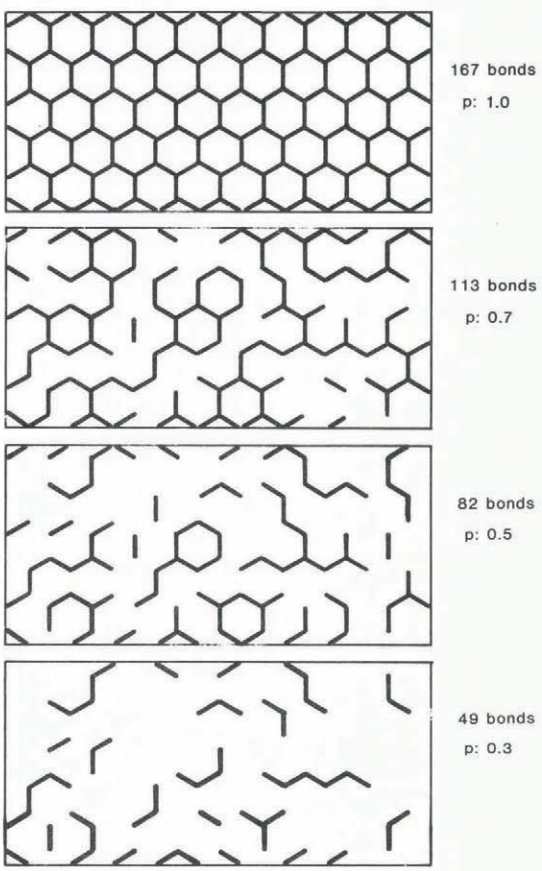

Fig.6. Two-dimensinal hexagonal lattice. Bonds have been eliminated according to random numbers.

$$\Pi = (\rho_i - \rho_f)/\rho_i \quad \Pi' = (\rho_i - \rho_f)/(\rho_i \cdot \rho_f) \qquad (6)$$

where: ρ_i = density of pure ice (0.919 Mg m^{-3})

ρ_f = bulk density of firn

Porosity Π is 0.20 m^3/m^3 for $\rho_f = 0.73$ Mg m^{-3}. If the critical percolation probability for the structure in question is $p_c = 0.42$, only 42% of the channels are still existing at the transition from firn to ice. This corresponds to a porosity of $\Pi = 0.084$ m^3/m^3 and a firn density of 0.840 Mg m^{-3}, which is in good agreement with the observations.

For finite samples all bonds connected to the surface of the sample contribute to the open pore volume, also if they would belong in the infinite sample to an isolated cluster of bonds. The porosity of a sample is given by the total number of existing bonds per volume, the bubble volume by the number of bonds which are not connected with the sample surface. The enclosure of bubbles can be simulated. More and more bonds of the three-dimensional structure are eliminated according to random numbers generated by the computer. The total number of bonds (corresponding to porosity) and the number of bonds not connected with the surface (corresponding to bubble volume) are counted in intervals.

The results of a computer simulation are shown in Figure 7. We started with 324, 1500, 4116 and 8748 bonds for the structure corresponding to a firn density of 0.73 Mg m^{-3}. A firn sample of 35 cm^3 at this density has about 30 000 channels. Channels in ice are not

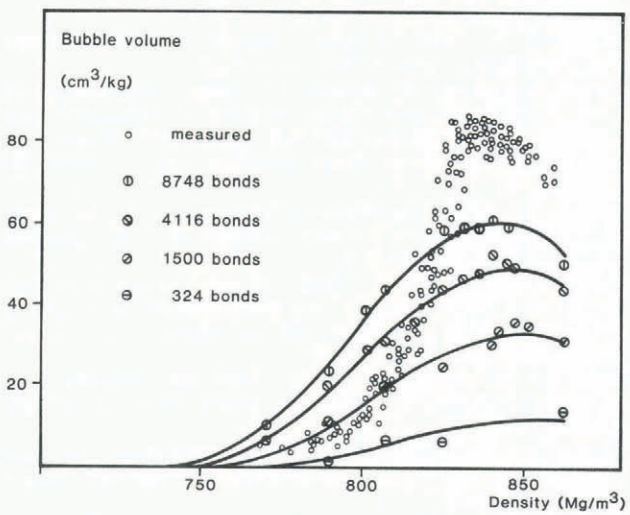

Fig.7. Enclosure of bubbles. Comparison of measured values with results from a simplified statistical model. The indicated number of bonds corresponds with the number of channels in a sample with the density 0.73 Mg m^{-3}.

eliminated any more as soon as they are enclosed, but they are shrinking, leading to a decrease of the bubble volume after completed close off. The computer simulation is not taking into account any shrinking of bonds, but isolated bonds are also allowed to be eliminated, which causes about the same effect.

The results of the simulation show the same trend as the measured values. The increase and absolute value of the bubble volume depends on sample size, respectively on the number of bonds. The model is in agreement with the observation that there are about two bubbles (bonds) per single crystal (tetrakaiderkaeder) at bubble close off, and that bubbles are often collected to small clusters.

ACKNOWLEDGEMENTS

This work has been supported by the Swiss National Science Foundation, by the DPP of US

https://doi.org/10.3189/1985AoG6-1-108-112 Published online by Cambridge University Press

National Science Foundation and the University of Bern. The ice core at Siple Station was drilled by the Polar Ice Coring Office, Nebraska.

REFERENCES

Anderson D L, Benson C S 1963 The densification and diagenesis of snow. *Ice and Snow*, MIT Press, Massachusetts, USA: 391-411

Beere W 1973 Energy considerations of intergranular pores and their relevance to gas release in fuels. *Physical Metallurgy of Reactor Fuel Elements*. Metals Society, London

Berner W, Stauffer B, Oeschger H 1979 Past, atmospheric composition and climate, gas parameters measured on ice cores. *Nature* 275(5683): 53-55

Coble R L 1961 Sintering crystalline solids. *Journal of Applied Physics* 32: 787-799

Desch C H 1919 The solidification of metals from the liquid state. *Journal of Instrumental Metallurgy* 22: 241-276

Delmas R J, Ascencio J M, Legrand M 1980 Polar ice evidence that atmospheric CO_2 20 000 years BP was 50% of present. *Nature* 284: 155-157

Essam J W 1980 Percolation theory. *Reports on Progress in Physics* 43: 833-912

Geguzin J E 1973 *Physik des Sinterns*. VEB Deutscher Verlag fur Grundstoffindustrie, Leipzig

Gow A J 1968 Bubbles and bubble pressure in Antarctic glacier ice. *Journal of Glaciology* 7(50): 167-182

Hammersley J M, Welsh D J A 1980 Percolation theory and its ramifications. *Contemporary Physics* 21(6): 593-605

Langway C C 1958 Physics of the movement of the ice. *IAHS Publication* 47: 336-349

Loosli H H 1983 A dating method with ^{39}Ar. *Earth and Planetary Science Letters* 63: 51-62

Maeno N, Narita M, Araoka K 1978 Measurements of air permeability and elastic modulus of snow and firn drilled at Mizuho Station East Antarctica. *Memoirs of National Institute of Polar Research* Special Issue 10: 62-76

Maeno N 1982 Densification rates of snow at polar glaciers. *Memoirs of National Institute of Polar Research* Special Issue 24: 204-211

Maeno N, Ebinuma T 1983 Pressure sintering of ice and its implication to the densification of snow at polar glaciers and ice sheets. *Journal of Physical Chemistry* 87(21): 4103-4110

Raynaud D, Lebel B 1979 Total gas content and surface elevation of polar ice sheets. *Nature* 281(5729): 289-291

Schwander J, Stauffer B 1985 Age difference between polar ice and the air trapped in its bubbles. *Nature* 315(6014): 45-47

Schwander J 1984 *Lufteinschluss im Eis von Groenland und der Antarktis*. (PhD thesis, University of Bern 1984)

Stauffer B, Berner W, Oeschger H, Schwander J 1981 Atmospheric CO_2 history from ice core studies. *Zeitschrift fur Gletscherkunde und Glazialgeologie* 17(1): 1-16

Stauffer B 1981 Mechanismen des Lufteinschlusses in natuerlichem Eis. *Zeitschrift fur Gletscherkunde und Glazialgeologie* 17(1): 17-56

Wilkinson D S, Ashby M F 1975 Pressure sintering by power law creep. *Acta Metallurgica* 23: 1277-1285